The Cushion Region and Dayside Magnetodisc Structure at Saturn

N. R. Staniland[1], M. K. Dougherty[1], A. Masters[1], and N. Achilleos[2]

[1]Blackett Laboratory, Imperial College London, London, UK
[2]Department of Physics and Astronomy, University College London, Gower St., London WC1E 6BT

Key Points:

- The first example of a cushion region at Saturn is identified
- Only five examples of a cushion are identified, showing this phenomenon to be rare, with four at dusk and one at dawn
- The dusk cushion could form due to the greater heating of plasma and the expansion of the field in the afternoon sector

Corresponding author: Ned Russell Staniland, `n.staniland17@imperial.ac.uk`

Abstract

A sustained quasi-dipolar magnetic field between the current sheet outer edge and the magnetopause, known as a cushion region, has previously been observed at Jupiter, but not yet at Saturn. Using the complete Cassini magnetometer data, the first evidence of a cushion region forming at Saturn is shown. Only five examples of a sustained cushion are found, revealing this phenomenon to be rare. Four of the cushion regions are identified at dusk and one pre-noon. It is suggested that greater heating of plasma post-noon coupled with the expansion of the field through the afternoon sector makes the disc more unstable in this region. These results highlight a key difference between the Saturn and Jupiter systems.

Plain Language Summary

1 Introduction

At the gas giants, the presence of an internal plasma source coupled with their rapid rotation ($\sim$ 10 hours) significantly perturbs their magnetic field configuration. Neutrals ejected from the moons Enceladus and Io in the inner magnetosphere of Saturn and Jupiter, respectively, become ionised, locking onto magnetic field lines and are accelerated towards corotation. The newly-formed plasma is centrifugally confined to the equator, radially stretching the magnetic field into a magnetodisc. This structure has been observed at all local times under expanded conditions at Saturn (Arridge, Russell, et al., 2008). At Jupiter, a region adjacent to the magnetopause where the magnetodisc structure breaks down and the field is quasi-dipolar, referred to as the "cushion region", has been identified (Went, Kivelson, et al., 2011) and is argued to be populated by mass-depleted flux tubes following tail reconnection (Kivelson & Southwood, 2005). However, this region has yet to be identified at Saturn (Went, Kivelson, et al., 2011), despite the similarities between these two systems.

At Saturn, mass that is loaded into the magnetosphere by Enceladus must be lost from the system. These water group ions (W^+) are eventually driven radially outwards in the low plasma beta ($\beta < 1$) inner magnetosphere via an interchange instability with the more tenuous hot plasma population in the outer magnetosphere (e.g. Gold (1959); Azari et al. (2018)). At larger radial distances, plasma pressure dominates ($\beta > 1$) and the magnetic field balloons until closed field lines reconnect and mass is lost in the magnetotail (Vasyliunas, 1983). Hence, mass-depleted flux tubes following nightside reconnection via this cycle, or the solar-wind driven Dungey cycle (Dungey, 1961), convect along the dawn flank towards noon and are subsequently refilled, thus restarting the mass transport cycle. It has been suggested that a turbulent channel of mass-depleted flux tubes should then reside radially outwards of the magnetodisc, where the field geometry is quasi-dipolar due to the lower mass content and a break down of the disc. This region is regarded as a signature of these cycles and has been identified at Jupiter (Kivelson & Southwood, 2005; Went, Kivelson, et al., 2011). However, since the arrival of Juno, Gershman et al. (2018) found there lacked a systematic cushion region at Jupiter, possibly highlighting that this dynamical picture is incomplete.

Supercorotating flow at dawn following Vasyliunas-type reconnection was identified at Saturn (Masters et al., 2011). Jasinski et al. (2019) identified a region of mass depleted flux tubes in the morning sector using the data from the CAPS Electron Spectrometer (ELS) instrument (Young et al., 2004). Yet a dipolar structure has not been seen in the magnetic field data (Went, Kivelson, et al., 2011). To identify whether the cushion is sustained over large scales, an analysis of how the global magnetic field structure varies with distance from the planet is required.

This study will use the complete Cassini orbital magnetometer dataset at Saturn (Dougherty et al., 2004) to show the first evidence of a cushion region at Saturn. This region is found to arise at dusk, rather than preferentially at dawn as was previously expected. We suggest that greater heating of the magnetodisc plasma at dusk compared to dawn (Kaminker et al., 2017) and the expansion of the magnetic field as it rotates through the afternoon sector produces these disc instabilities.

2 Data Selection

To search for a cushion region at Saturn, all Cassini orbits that traversed the dayside inner magnetosphere out to the magnetopause, whilst remaining near the equator ($\pm 30°$) are analysed to track changes in the magnetic field configuration. Crossings of the dayside magnetopause are identified using the Jackman et al. (2019) catalogue. The nose standoff distance R_{SS} for each unique crossing, using the crossing closest to the planet if there are multiple during a single traversal, is mapped with the Pilkington et al. (2015) dawn-dusk asymmetric magnetopause model. The 92 suitable revolutions (Revs) that fulfil the above criteria are shown in Figure 1.

The 1-minute resolution magnetometer data is transformed into Kronocentric Solar Magnetic (KSMAG) spherical coordinates, where r is the radial component and positive pointing away from Saturn, θ is the meridional component and ϕ is the azimuthal component increasing in the direction of rotation. An 11-hour (approximate rotation period) sliding average of the data is taken to focus on the global structure and filter other variability, including the ubiquitous planetary period oscillations (PPOs) (see Carbary and Mitchell (2013) review and references therein).

3 Finding the Cushion Region

To identify whether a cushion exists, there must be a stable disc structure in the middle magnetosphere, otherwise the field could be quasi-dipolar everywhere. There are two conditions for the field to be disc-like (Went, Kivelson, et al., 2011). Firstly, the field must be predominantly radial such that $B_r^2/B^2 > B_\theta^2/B^2$. These ratios are shown in panels b) and e) of Figure 2. However, this criterion is insufficient when Cassini is away from the equator, where a dipole field is not purely north-south. This is particularly important to consider if the current sheet is warped (Arridge, Khurana, et al., 2008). To account for this, the second criterion is for the angle between the measured magnetic field and a dipole, where we have used the Dougherty et al. (2018) model, to be $90 \pm 30°$. This angle is shown in panels c) and f) of Figure 2. When both these criteria are satisfied, the field is disk-like.

The location 80% of the distance from the $15R_S$ disc inner edge to the magnetopause is set as the cushion region inner edge. For instance, if the magnetopause radial position is $r = 25R_S$ the cushion inner edge is $r = 23R_S$. Whilst this is closer to the magnetopause than the average inner boundary of the Jovian cushion (Went, Kivelson, et al., 2011), it is chosen due to the lack of an observed cushion thus far and the smaller magnetosphere of Saturn. It is also far enough from the magnetopause to assume we are not measuring the shielding of the field by the boundary currents, although there is previous evidence of the disc persisting up to the magnetopause (Arridge, Russell, et al., 2008) shows that this effect should be negligible. We then calculate what percentage of the data fulfil the two criteria in the disc region (from $15R_S$ to the cushion inner edge). If it is more than 50%, we suggest that there exists a stable magnetodisc structure. In the remaining layer up to the magnetopause, if this percentage remains approximately constant, the field is still disc-like. If the percentage significantly reduces and the field becomes more dipolar, there is a cushion. If less than 50% of the disc region has fulfilled the criteria, there is no stable magnetodisc and hence no cushion. This ensures we see two distinct regions with persistent and sustained structures.

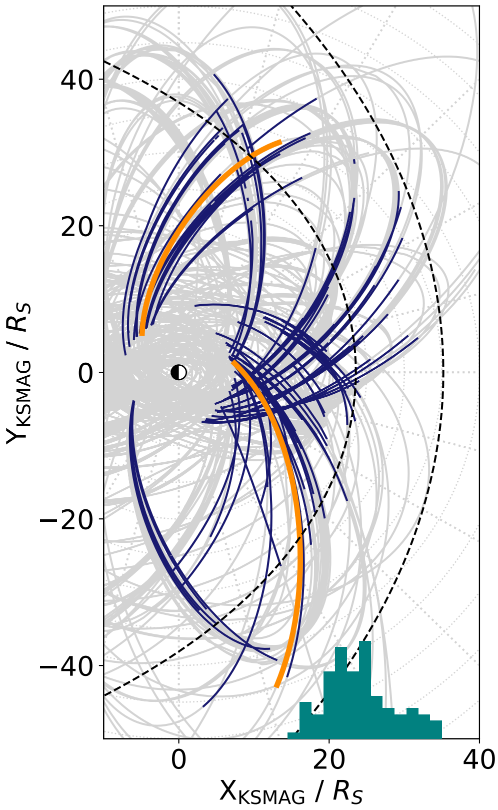

Figure 1. The complete Cassini orbital mission trajectory is shown in light grey, projected onto the equatorial plane. The trajectory of Cassini during the 92 Revs used in this study is shown in dark blue. The orange trajectories show the case studies in Figure 2. Magnetopause (Pilkington et al., 2015) and bow shock (Went, Hospodarsky, et al., 2011) models, assuming solar wind dynamic pressure of 0.01 nPa, are shown with black dashed curves. The histogram shows R_{SS} for each crossing.

The change in percentage across these two regions for all 92 Revs was calculated. The mean was a reduction by $\mu = 6\%$ with a standard deviation of $\sigma = 24\%$. We define those Revs whose reduction in percentage is greater than $\mu + 2\sigma = 54\%$ as having a cushion. This is large enough to consider these as examples of a cushion and not an artefact of our method compared to if, for instance, $\mu + 2\sigma$ was only 10%.

3.1 Results

For Rev 20 in Figure 2, the disc criteria are satisfied for 97% of the disc region and for 100% of the cushion region, showing an example of a stable magnetodisc structure that persists up to the magnetopause. The mapped standoff distance R_{SS} for Rev 20 was $32R_S$, showing that the system was significantly expanded. For Rev 168, the criteria are satisfied for 66% of the disc region. However, the percentage drops to just 2% in the cushion region and the field becomes significantly more dipolar. For Rev 168, $R_{SS} = 26R_S$, showing the system was expanded. We suggest that this is the first evidence of a cushion region observed at Saturn.

A potential explanation for the Rev 168 cushion region could be that the dipolar outer boundary reflects the change in local time as Cassini moves away from noon (in

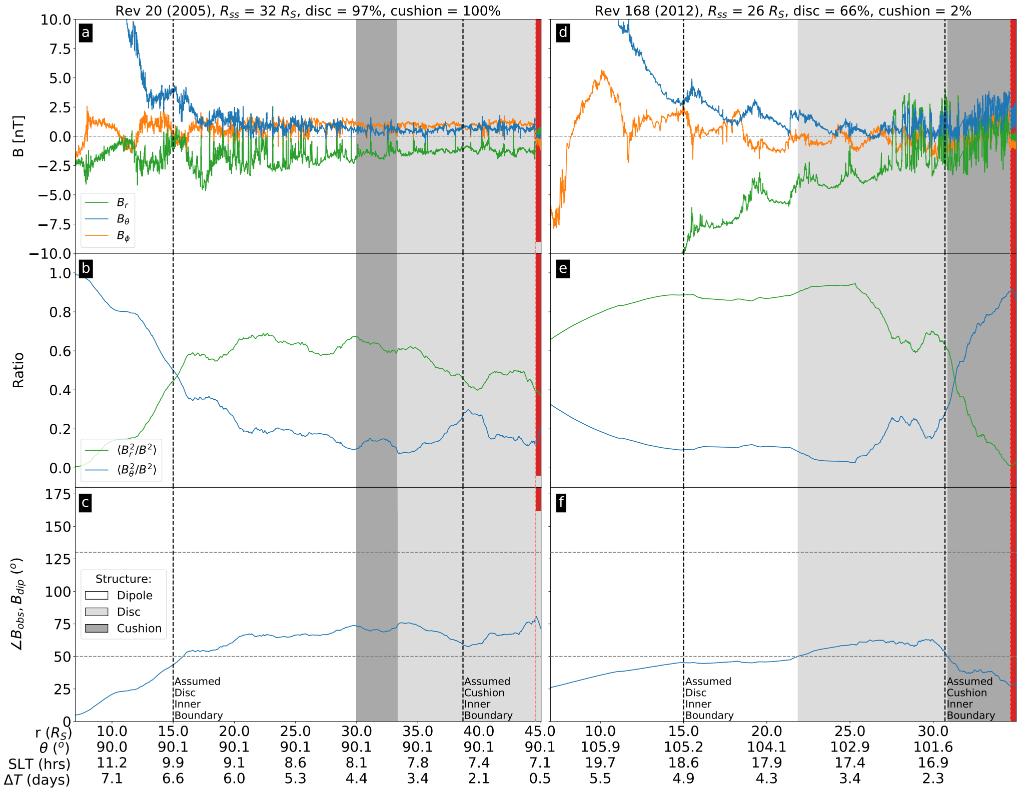

Figure 2. Two examples of Cassini traversing the equatorial dayside magnetosphere are shown as a function of radial distance. The top panels show the 1-minute resolution field data in spherical coordinates. The second panels show the ratio of the 11-hour smoothed radial and meridional components to the total field. The bottom panels show the angle between the measured field and the Dougherty et al. (2018) model. These identify the structure of the field. The panels are shaded to show if the field is dipole-like (white), disc-like (light grey), cushion-like (dark grey), or in the magnetosheath (red). The assumed disc and cushion region boundaries are shown as vertical dashed lines. The left panels show an example at dawn where the magnetodisc is present up until the magnetopause, whilst the right panels show an example at dusk where a cushion is identified. At the bottom of the figure the radial distance (r), co-latitude (θ), Saturn local time (SLT), and ΔT are shown.

time) and the magnetopause confinement of the field reduces. However, Cassini only passed through 0.2 hours of local time in the cushion region, and 1.2 hours between where the disc was first observed and the cushion region inner edge, producing a small change in the magnetopause radial position. In addition, Revs with a similar noonward trajectory where a disc was observed at dawn did not observe a dipolar outer region. Another explanation could be that the magnetosphere underwent a sudden solar wind compression. Whilst for the Rev 168 there is a small increase in magnetic field strength (∼1 nT), the data are particularly noisy in this region and the cushion was observed radially inwards of this small increase. In addition, we compared the field profile for all five potential examples of a cushion region (see Figure 3) and saw no significant increase in field strength to suggest that these are results of a solar wind compression.

This analysis was carried out for all 92 Revs. Only 15 Revs had a sustained magnetodisc and are shown in Figure 3a) in grey. The disc formed not only when the magnetosphere was expanded ($R_{SS} > 23R_S$), but even when R_{SS} was as low as $17R_S$. Of these 15 Revs, five have examples of cushion regions and are highlighted in Figure 3a). For all cushion region examples $R_{SS} > 23R_S$. However, a cushion does not arise whenever the magnetosphere is expanded. In particular, it does not arise preferentially at dawn as was expected.

In panel b) of Figure 3, the average magnetic field structure calculated using this subset of 15 Revs with a sustained magnetodisc is shown, revealing a local time asymmetry in our dataset. When there is a magnetodisc at dawn, the structure is stable in the disc region (median of 95% for nine Revs) and this continues into the presumed cushion region (median of 100%). At dusk, when there is a magnetodisc it is on average less stable in the disc region (median of 68% for six Revs) and this significantly drops in the cushion region (median of 1%). There are two examples of a stable disc that persists up to the magnetopause at dusk, compared to eight at dawn. If we use the mean percentage for Figure 3b), the one cushion example at dawn makes the cushion region a darker green. However, due to the small number of examples in our dataset the median is used instead.

We can analyse whether the dawn-dusk asymmetry observed is statistically significant. We only include Revs where $R_{SS} > 23R_S$ since disc formation depends on system size. We use the Fisher's exact test to test the null hypothesis that cushion formation is local time symmetric. We find that the cushion local time asymmetry was not found to be statistically significant ($p \gg 0.05$ for all choices of R_{SS}). Nonetheless, even a few cases of a dusk cushion suggests that it it cannot be a return flow channel related to tail reconnection. Another formation mechanism is required.

For this study, the focus is on whether a significant portion of the outer boundary is quasi-dipolar, reflective of the cushion region that has been observed at Jupiter, rather than being intermittently dipolar. We have taken an 11-hour average of the magnetic field data to focus on the large-scale properties of the magnetic field structure. Some examples of an intermittent cushion were therefore removed from our analysis. We found that the overall structure at dusk is far noisier, which is reflected in the low disc region percentage at dusk in Figure 3.

4 Discussion

The magnetodisc structure maintains an equilibrium between the outward directed centrifugal force, the magnetic and plasma pressures, and the magnetic field tension in the curved geometry that provides the inward centripetal force required to enforce subcorotation. The field radius of curvature R_C supports this equilibrium. Magnetodisc break down can occur when this radial stress balance is disrupted and the magnetic field can no longer contain the plasma. Ballooning of the disc occurs when the plasma parallel pressure is greater than the perpendicular pressure plus the magnetic tension associated with the curved field geometry. This instability can lead to reconnection and plasma breaking off the disc. To identify where force balance in the disc might break down, we can compare the gyoradii of heavy ions in each local time sector to identify where it approaches R_C. The typical ion gyroradius of a charged particle can be expressed as

$$r_i = \frac{\sqrt{2mk_bT}}{|q|B} \tag{1}$$

where m is the particle mass, q is the charge, B is the local magnetic field strength, T is the temperature (where we assume that $T_\perp \approx T$) and where k_b is the Boltzmann constant. Went, Kivelson, et al. (2011) calculated the critical density of the disc under which stress balance would break down. However, due to a lack of data close to the magnetopause at Saturn they could not resolve whether the critical density approached the current sheet

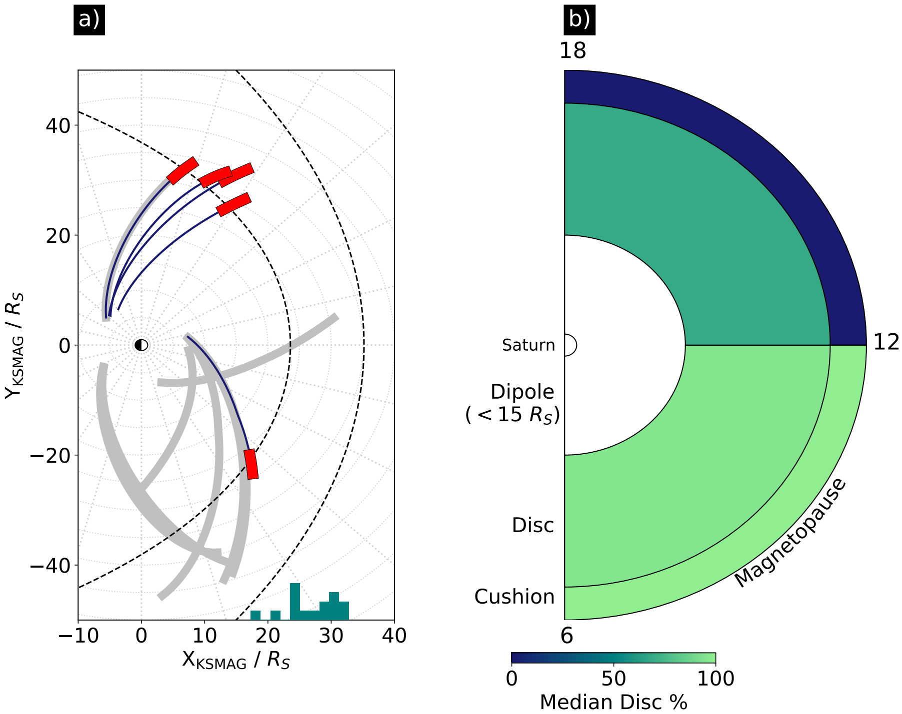

Figure 3. Panel a) shows the 15 Cassini Revs where a stable disc was identified. The five cushion examples are shown in blue, with the cushion highlighted in red. Panel b) shows a representation of the average dayside configuration calculated using the 15 examples in panel a). The three radial sectors of dipole, disc, and cushion are labelled and the dayside is divided into dawn and dusk local time sectors, with the 15 Cassini Revs categorised by the local time position of the magnetopause crossing. The colorbar shows the median disc percentage. There is a distinct disc structure at dawn that persists up to the magnetopause (light green). At dusk, on average there is a less stable disc in the disc region (dark green) and the field becomes more dipolar in the cushion region (blue).

density in the outer magnetosphere. Now the Cassini mission is complete, we can build on their work using the latest results to understand these new cushion observations.

The Jackman et al. (2019) catalogue is used to determine when Cassini is within the magnetosphere. A mean equatorial ($\pm 20^o$) magnetic field strength radial profile for the dawn (6-12 LT) and dusk (12-18 LT) sectors is calculated, as well as profiles $\pm 1\sigma$ from the mean to capture the variability. The average value of R_{SS} for our five cushion region examples is 25.9 R_S.

An unexpected observation at Saturn is the increasing temperature of thermal ions with radial distance. Turbulent heating driven by oppositely directed Alfvén waves interacting could explain this phenomenon (Saur, 2004; Saur et al., 2018; Papen et al., 2014). From fluctuations in the magnetic field, Kaminker et al. (2017) calculated the heating rate density q of plasma due to turbulence. They found a quiet region between 3-9 LT and an active region between 10-20 LT with an average two orders of magnitude difference in q. We use the Ng et al. (2018) advective turbulent heating model based to calculate the ion temperature, similar to Neupane et al. (2021) but incorporating a local time asymmetry. The temperature is given by

$$T = T_0 \left(\frac{L}{L_0}\right)^{-2\beta/3} + c_1 \left(\frac{L}{L_0}\right)^{-2\beta/3} \int_{L_0}^{L} q(L') \frac{L'^{\alpha+2\beta/3}}{L_0^{2\beta/3}} \mathrm{d}L' \quad (2)$$

where $L_0 = 8R_S$, T_0 is the average temperature at $8R_S$ Wilson et al. (2017), and $c_1 = \frac{2R_S^3 2\pi m_i H}{3\dot{M} k_b}$ where $m_i = 16$ amu for W^+ ions, $H = 1.6R_S$ is the current sheet thickness (Staniland et al., 2020) and $\dot{M} = 50$ kg is the mass transport rate Neupane et al. (2021). We fix the parameters for both local time sectors but vary q based on Kaminker et al. (2017) such that $q \sim 10^{-16}$ W/m^3 at dusk and $q \sim 10^{-18}$ W/m^3 at dawn.

Plugging these into Equation 1, we get one-dimensional gyroradii profiles as a function of radial distance shown in Figure 4. At dawn, the gyoradius increases from $\sim 10^1$km in the inner magnetosphere, to 10^2km close to the nose standoff distance, and finally to 10^3km at the terminator. At dusk, the gyoradius is larger due to the higher temperature, reaching 10^4km at the terminator.

To calculate R_C at Saturn, we use the AGA/UCL Magnetodisc Model (Achilleos et al., 2010) assuming an average hot plasma index of $K_h = 2e6$ Pa m, where K_h is essentially a measure of the ring current activity. The smallest value of R_C calculated in the model was $\sim 0.70R_S$.

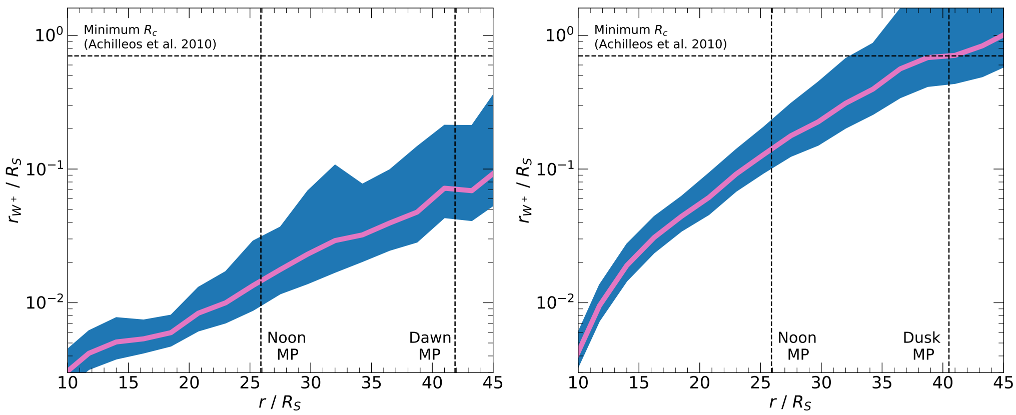

Figure 4. The water group ion gyoradius r_{W+} is shown as a function of radial distance for the dawn (left) and dusk (right) local time sectors. The horizontal dashed lines show the minimum expected radius of curvature. The vertical dashed lines show the average nose standoff distance for our five cushion examples and the mapped terminators. The pink line shows r_{W+} calculated using the average magnetic field strength. The blue region shows r_{W+} calculated using the standard deviations of the mean magnetic field. These results show that r_{W+} approaches R_C at dusk at distances between noon and the terminator, but at dawn it far less likely to.

Figure 4 shows that at dawn, due to the lower temperature the gyroadius remains smaller than the minimum expected radius of curvature associated with the magnetodisc geometry. At dusk, due to the greater heating rate density, the ion gyroradius is more likely to approach magnetodisc curvature length-scales in the outer magnetosphere. Past this region, the magnetohydrodynamic approximation of the magnetodisc breaks down and force balance is no longer maintained. Kaminker et al. (2017) have shown that the whilst the average heating rate density measured at dusk is larger than at dawn, it is also more variable, indicative of spot heating and spatially intermittent turbulence. This could explain why the cushion is not systematically at dusk and instead arises infrequently.

Delamere et al. (2015) found evidence of mass being lost from the disc through signatures of reconnection, given by $B_\theta < 0$, predominantly in the subsolar to dusk regions. They suggest a circulation pattern in the magnetodisc where mass is lost through patchy reconnection in the dusk flank, rather than through large-scale tail reconnection. In our study, whilst we have observed large-scale cushion regions forming at dusk, they are rare. We suggest that the intermittent signatures of a cushion and the patchy reconnection observed at dusk by Delamere et al. (2015) are probably more typical. As flux tubes rotates through dusk they are able to expand since the magnetopause no longer confines the field, resulting in a centrifugally driven increase in the parallel pressure of the plasma. This triggers an anisotropy ($T_\parallel > T_\perp$) that results in the disc becoming explosively unstable at dusk (Kivelson & Southwood, 2005). There could also be a further role of the solar wind and the Dungey cycle (Dungey, 1961) in the dusk cushion formation, as well as the planetary period oscillations that thin the current sheet (Cowley et al., 2017). At Jupiter, the presence of a statistical reconnection x-line across the tail (Vogt et al., 2010), compared to the patchy reconnection observed at Saturn, could further highlight why the systematic cushion at Jupiter is well-described as a return flow channel following tail reconnection, but the Saturn cushion region is not.

The suprathermal plasma population within the magnetosphere of Saturn could also play a role in cushion formation. These particles are more mobile and gyrate further up the magnetic field. The energetic particles and distribution of suprathermal pressure can help to maintain a quasi-dipolar field in the outer magnetosphere. At the same time, the suprathermal plasma can act to inflate the radially stretched flux tubes in the disc region. The suprathermal plasma can exert anisotropic pressure, with $p_\parallel > p_\perp$, adding to the disc-like configuration of the field. This could drive a ballooning instability, leading to magnetodisc break down. There is also an asymmetry in the hot plasma pressure, which is larger at dusk compared to dawn (Sergis et al., 2017; Sorba et al., 2019), that could motivate disc break down in this region.

Pulsations in the ultraviolet (UV) auroral emissions have further been linked with magnetodisc reconnection and are observed to preferentially occur at dusk with patchy, diffuse signatures (Bader et al., 2019, 2020). These phenomena highlight the quieter dawn magnetodisc that maps to the aurora along field-aligned currents compared to the active and more variable dusk magnetodisc and cushion that generate these structures.

5 Conclusion

Using the complete Cassini orbital magnetometer dataset, we have identified five examples of a cushion region at Saturn, of which four were observed at dusk. These results are in contrast with the current interpretation of a cushion that suggests it is a return flow channel of mass depleted flux tubes following tail reconnection. We argue that due to a local time asymmetry in the heating of the plasma and the expansion of the field as the plasma moves through the afternoon sector, the disc at dusk can break down, allowing for a cushion region to form in this local time sector. The difference in local time distribution coupled with the lack of cushion examples at Saturn reveals a key difference compared to Jupiter, where the cushion forms at dawn and is driven by nightside reconnection.

Acknowledgments

N. R. S. is funded by the STFC DTP Studentship. M. K. D. is supported by a Royal Society Research Professorship. A. M. is supported by a Royal Society University Research Fellowship. N. A. was supported by the UK STFC Consolidated Grant (UCL/MSSL Solar and Planetary Physics, ST/N000722/1). Cassini magnetic field data are available at NASA's Planetary Data System (PDS) (https://pds-ppi.igpp.ucla.edu/) in the folder

CO-E/SW/J/SMAG-4-SUMM-1MINAVG-V2.0. We would like to thank David Southwood for his insightful discussions.

References

Achilleos, N., Guio, P., & Arridge, C. S. (2010, Feb). A model of force balance in saturn's magnetodisc. *Monthly Notices of the Royal Astronomical Society*, *401*(4), 2349–2371. Retrieved from `http://dx.doi.org/10.1111/j.1365-2966.2009.15865.x` doi: 10.1111/j.1365-2966.2009.15865.x

Arridge, C. S., Khurana, K. K., Russell, C. T., Southwood, D. J., Achilleos, N., Dougherty, M. K., ... Leinweber, H. K. (2008). Warping of Saturn's magnetospheric and magnetotail current sheets. *Journal of Geophysical Research: Space Physics*, *113*(8), 1–13. doi: 10.1029/2007JA012963

Arridge, C. S., Russell, C. T., Khurana, K. K., Achilleos, N., Cowley, S. W., Dougherty, M. K., ... Bunce, E. J. (2008). Saturn's magnetodisc current sheet. *Journal of Geophysical Research: Space Physics*, *113*(4), 1–9. doi: 10.1029/2007JA012540

Azari, A. R., Liemohn, M. W., Jia, X., Thomsen, M. F., Mitchell, D. G., Sergis, N., ... Vandegriff, J. (2018). Interchange Injections at Saturn: Statistical Survey of Energetic H+ Sudden Flux Intensifications. *Journal of Geophysical Research: Space Physics*, *123*(6), 4692–4711. doi: 10.1029/2018JA025391

Bader, A., Badman, S. V., Yao, Z. H., Kinrade, J., & Pryor, W. R. (2019). Observations of Continuous Quasiperiodic Auroral Pulsations on Saturn in High Time-Resolution UV Auroral Imagery. *Journal of Geophysical Research: Space Physics*, *124*(4), 2451–2465. doi: 10.1029/2018JA026320

Bader, A., Cowley, S. W., Badman, S. V., Ray, L. C., Kinrade, J., Palmaerts, B., & Pryor, W. R. (2020). The Morphology of Saturn's Aurorae Observed During the Cassini Grand Finale. *Geophysical Research Letters*, *47*(2). doi: 10.1029/2019GL085800

Carbary, J. F., & Mitchell, D. G. (2013). Periodicities in saturn's magnetosphere. *Reviews of Geophysics*, *51*(1), 1-30. Retrieved from `https://agupubs.onlinelibrary.wiley.com/doi/abs/10.1002/rog.20006` doi: 10.1002/rog.20006

Cowley, S. W., Provan, G., Hunt, G. J., & Jackman, C. M. (2017). Planetary period modulations of Saturn's magnetotail current sheet: A simple illustrative mathematical model. *Journal of Geophysical Research: Space Physics*, *122*(1), 258–279. doi: 10.1002/2016JA023367

Delamere, P. a., Otto, a., Ma, X., Bagenal, F., & Wilson, R. J. (2015). Journal of Geophysical Research : Space Physics Magnetic flux circulation in the rotationally driven giant magnetospheres. , 4229–4245. doi: 10.1002/2015JA021036.Received

Dougherty, M., Cao, H., Khurana, K., Hunt, G., Provan, G., Kellock, S., ... Southwood, D. (2018). Saturn's magnetic field revealed by the cassini grand finale (vol 362, eaat5434, 2018). *SCIENCE*, *362*. Retrieved from `http://dx.doi.org/10.1126/science.aav6732` doi: 10.1126/science.aav6732

Dougherty, M., Kellock, S., Southwood, D. J., Balogh, A., Smith, E. J., Tsurutani, B. T., ... Cowley, S. W. H. (2004). The Cassini Magnetic Field Investigation. *The Cassini-Huygens Mission*, 331–383. Retrieved from `http://link.springer.com/10.1007/978-1-4020-2774-1{\_}4` doi: 10.1007/978-1-4020-2774-1_4

Dungey, J. W. (1961). Interplanetary magnetic field and the auroral zones. *Physical Review Letters*, *6*(2), 47–48. doi: 10.1103/PhysRevLett.6.47

Gershman, D. J., DiBraccio, G. A., Connerney, J. E., Bagenal, F., Kurth, W. S., Hospodarsky, G. B., ... Bolton, S. J. (2018). Juno Constraints on the Formation of Jupiter's Magnetospheric Cushion Region. *Geophysical Research*

Letters, *45*(18), 9427–9434. doi: 10.1029/2018GL079118

Gold, T. (1959). Motions in the magnetosphere of the earth. *Journal of Geophysical Research (1896-1977)*, *64*(9), 1219-1224. Retrieved from `https://agupubs.onlinelibrary.wiley.com/doi/abs/10.1029/JZ064i009p01219` doi: 10.1029/JZ064i009p01219

Jackman, C. M., Thomsen, M. F., & Dougherty, M. K. (2019). Survey of Saturn's Magnetopause and Bow Shock Positions Over the Entire Cassini Mission: Boundary Statistical Properties and Exploration of Associated Upstream Conditions. *Journal of Geophysical Research: Space Physics*, *124*(11), 8865–8883. doi: 10.1029/2019JA026628

Jasinski, J. M., Arridge, C. S., Bader, A., Smith, A. W., Felici, M., Kinrade, J., ... Murphy, N. (2019). Saturn's Open-Closed Field Line Boundary: A Cassini Electron Survey at Saturn's Magnetosphere. *Journal of Geophysical Research: Space Physics*, *124*(12), 10018–10035. doi: 10.1029/2019JA027090

Kaminker, V., Delamere, P. A., Ng, C. S., Dennis, T., Otto, A., & Ma, X. (2017). Local time dependence of turbulent magnetic fields in Saturn's magnetodisc. *Journal of Geophysical Research: Space Physics*, *122*(4), 3972–3984. doi: 10.1002/2016JA023834

Kivelson, M. G., & Southwood, D. J. (2005). Dynamical consequences of two modes of centrifugal instability in Jupiter's outer magnetosphere. *Journal of Geophysical Research: Space Physics*, *110*(A12). doi: 10.1029/2005JA011176

Masters, A., Thomsen, M. F., Badman, S. V., Arridge, C. S., Young, D. T., Coates, A. J., & Dougherty, M. K. (2011). Supercorotating return flow from reconnection in Saturn's magnetotail. *Geophysical Research Letters*, *38*(3), 3–7. doi: 10.1029/2010GL046149

Neupane, B. R., Delamere, P. A., Ma, X., Ng, C., Burkholder, B., & Damiano, P. (2021). On The Nature of Turbulent Heating and Radial Transport in Saturn's Magnetosphere. *Journal of Geophysical Research: Space Physics*, *126*(1), 1–15. doi: 10.1029/2020ja027986

Ng, C. S., Delamere, P. A., Kaminker, V., & Damiano, P. A. (2018). Radial Transport and Plasma Heating in Jupiter's Magnetodisc. *Journal of Geophysical Research: Space Physics*, *123*(8), 6611–6620. doi: 10.1029/2018JA025345

Papen, M. V., Saur, J., & Alexandrova, O. (2014). Journal of Geophysical Research : Space Physics Turbulent magnetic field fluctuations in Saturn ' s magnetosphere. *Journal of Geophysical Research: Space Physics*, *119*, 2797–2818. doi: 10.1002/2013JA019542.Received

Pilkington, N. M., Achilleos, N., Arridge, C. S., Guio, P., Masters, A., Ray, L. C., ... Dougherty, M. K. (2015). Asymmetries observed in Saturn's magnetopause geometry. *Geophysical Research Letters*, *42*(17), 6890–6898. doi: 10.1002/2015GL065477

Saur, J. (2004, feb). Turbulent heating of jupiter's middle magnetosphere. *The Astrophysical Journal*, *602*(2), L137–L140. Retrieved from `https://doi.org/10.1086%2F382588` doi: 10.1086/382588

Saur, J., Janser, S., Schreiner, A., Clark, G., Mauk, B. H., Kollmann, P., ... Kotsiaros, S. (2018). Wave-Particle Interaction of Alfvén Waves in Jupiter's Magnetosphere: Auroral and Magnetospheric Particle Acceleration. *Journal of Geophysical Research: Space Physics*, *123*(11), 9560–9573. Retrieved from `https://doi.org/10.1029/2018JA025948` doi: 10.1029/2018JA025948

Sergis, N., Jackman, C. M., Thomsen, M. F., Krimigis, S. M., Mitchell, D. G., Hamilton, D. C., ... Wilson, R. J. (2017). Radial and local time structure of the Saturnian ring current, revealed by Cassini. *Journal of Geophysical Research: Space Physics*, *122*(2), 1803–1815. doi: 10.1002/2016JA023742

Sorba, A. M., Achilleos, N. A., Sergis, N., Guio, P., Arridge, C. S., & Dougherty, M. K. (2019). Local time variation in the large-scale structure of saturn's magnetosphere. *Journal of Geophysical Research: Space Physics*, *124*(9), 7425-

7441. Retrieved from https://agupubs.onlinelibrary.wiley.com/doi/abs/10.1029/2018JA026363 doi: 10.1029/2018JA026363

Staniland, N. R., Dougherty, M. K., Masters, A., & Bunce, E. J. (2020). Determining the Nominal Thickness and Variability of the Magnetodisc Current Sheet at Saturn. *Journal of Geophysical Research: Space Physics*, *125*(5), 1–15. doi: 10.1029/2020JA027794

Vasyliunas, V. M. (1983). Plasma distribution and flow. In *Physics of the jovian magnetosphere* (p. 395-453). Cambridge University Press. doi: 10.1017/CBO9780511564574.013

Vogt, M. F., Kivelson, M. G., Khurana, K. K., Joy, S. P., & Walker, R. J. (2010). Reconnection and flows in the jovian magnetotail as inferred from magnetometer observations. *Journal of Geophysical Research: Space Physics*, *115*(A6). Retrieved from https://agupubs.onlinelibrary.wiley.com/doi/abs/10.1029/2009JA015098 doi: https://doi.org/10.1029/2009JA015098

Went, D. R., Hospodarsky, G. B., Masters, A., Hansen, K. C., & Dougherty, M. K. (2011). A new semiempirical model of Saturn's bow shock based on propagated solar wind parameters. *Journal of Geophysical Research: Space Physics*, *116*(7), 1–9. doi: 10.1029/2010JA016349

Went, D. R., Kivelson, M. G., Achilleos, N., Arridge, C. S., & Dougherty, M. K. (2011). Outer magnetospheric structure: Jupiter and Saturn compared. *Journal of Geophysical Research: Space Physics*, *116*(4), 1–14. doi: 10.1029/2010JA016045

Wilson, R. J., Bagenal, F., & Persoon, A. M. (2017). Survey of thermal plasma ions in Saturn's magnetosphere utilizing a forward model. *Journal of Geophysical Research: Space Physics*, *122*(7), 7256–7278. doi: 10.1002/2017JA024117

Young, D. T., Berthelier, J. J., Blanc, M., Burch, J. L., Coates, A. J., Goldstein, R., . . . Zinsmeyer, C. (2004, Sep 01). Cassini plasma spectrometer investigation. *Space Science Reviews*, *114*(1), 1–112. Retrieved from https://doi.org/10.1007/s11214-004-1406-4 doi: 10.1007/s11214-004-1406-4

Figure 1.

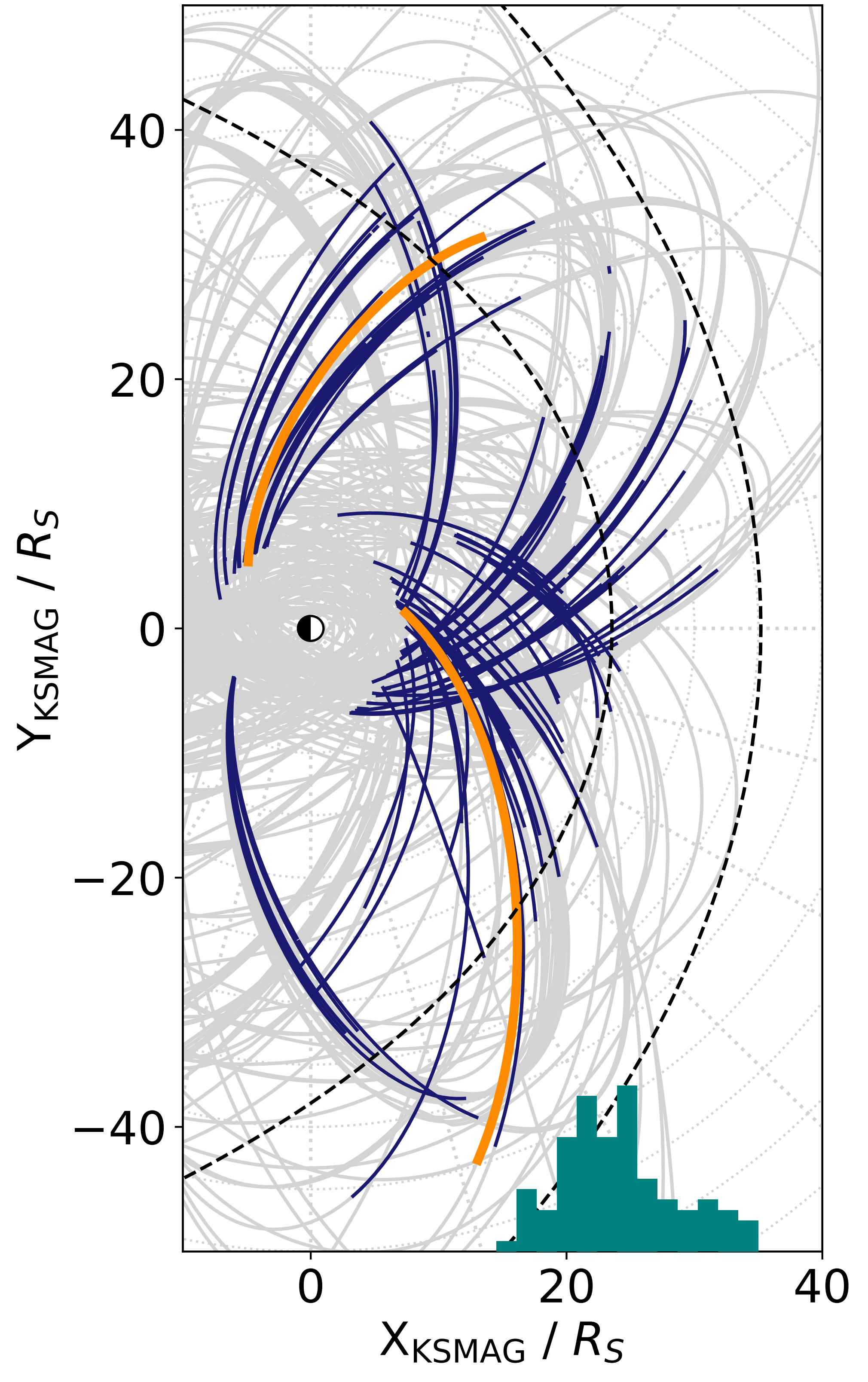

40
20
0
−20
−40
0
20
40
Y_{KSMAG} / R_S
X_{KSMAG} / R_S

Figure 2.

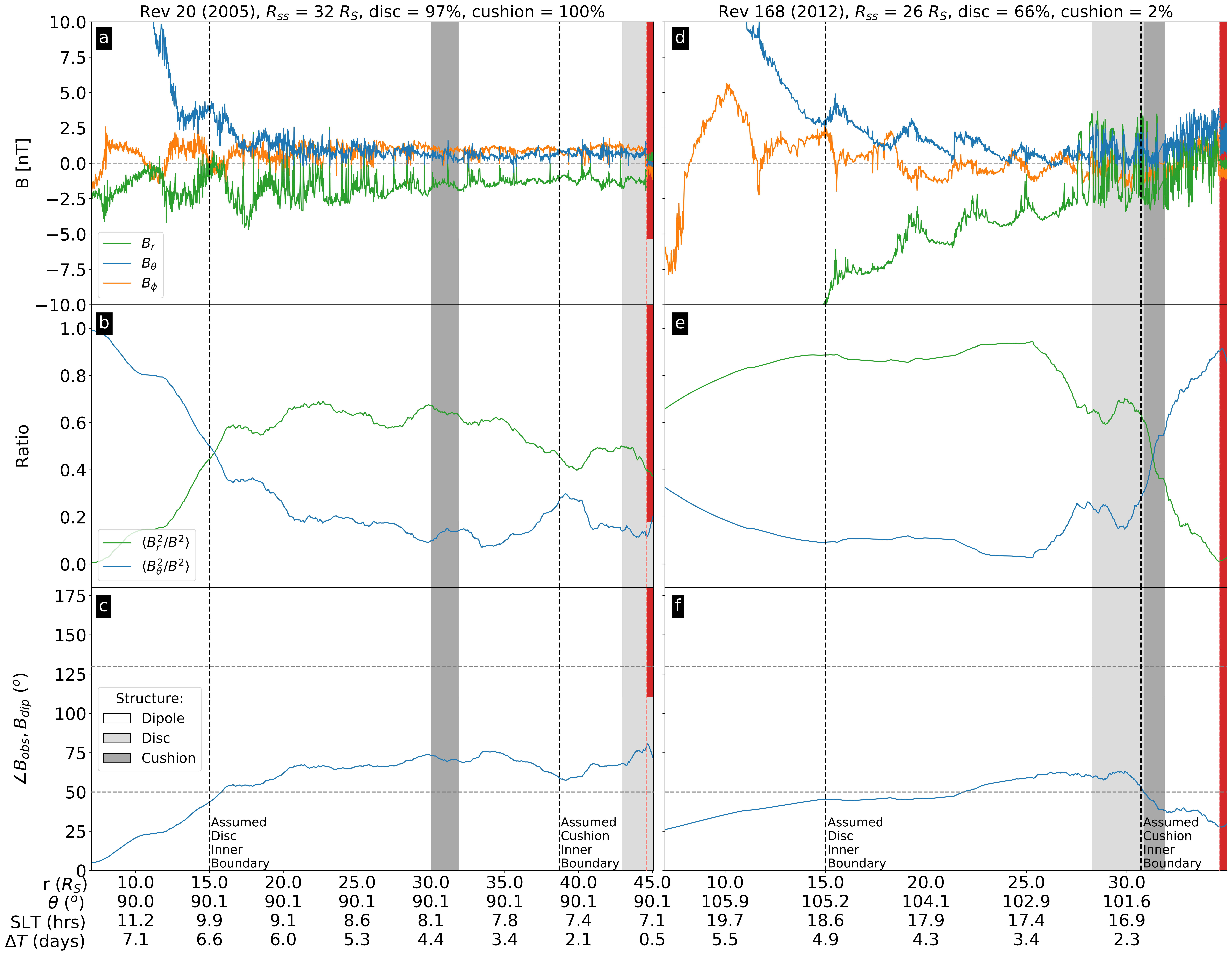

Rev 20 (2005), R_{ss} = 32 R_S, disc = 97%, cushion = 100%
Rev 168 (2012), R_{ss} = 26 R_S, disc = 66%, cushion = 2%
a
b
c
d
e
f
B [nT]
Ratio
$\angle B_{obs}, B_{dip}$ (^{o})
B_r
B_θ
B_ϕ
$\langle B_r^2/B^2 \rangle$
$\langle B_\theta^2/B^2 \rangle$
Structure:
Dipole
Disc
Cushion
Assumed Disc Inner Boundary
Assumed Cushion Inner Boundary
r (R_S)
θ (^{o})
SLT (hrs)
ΔT (days)

Figure 3.

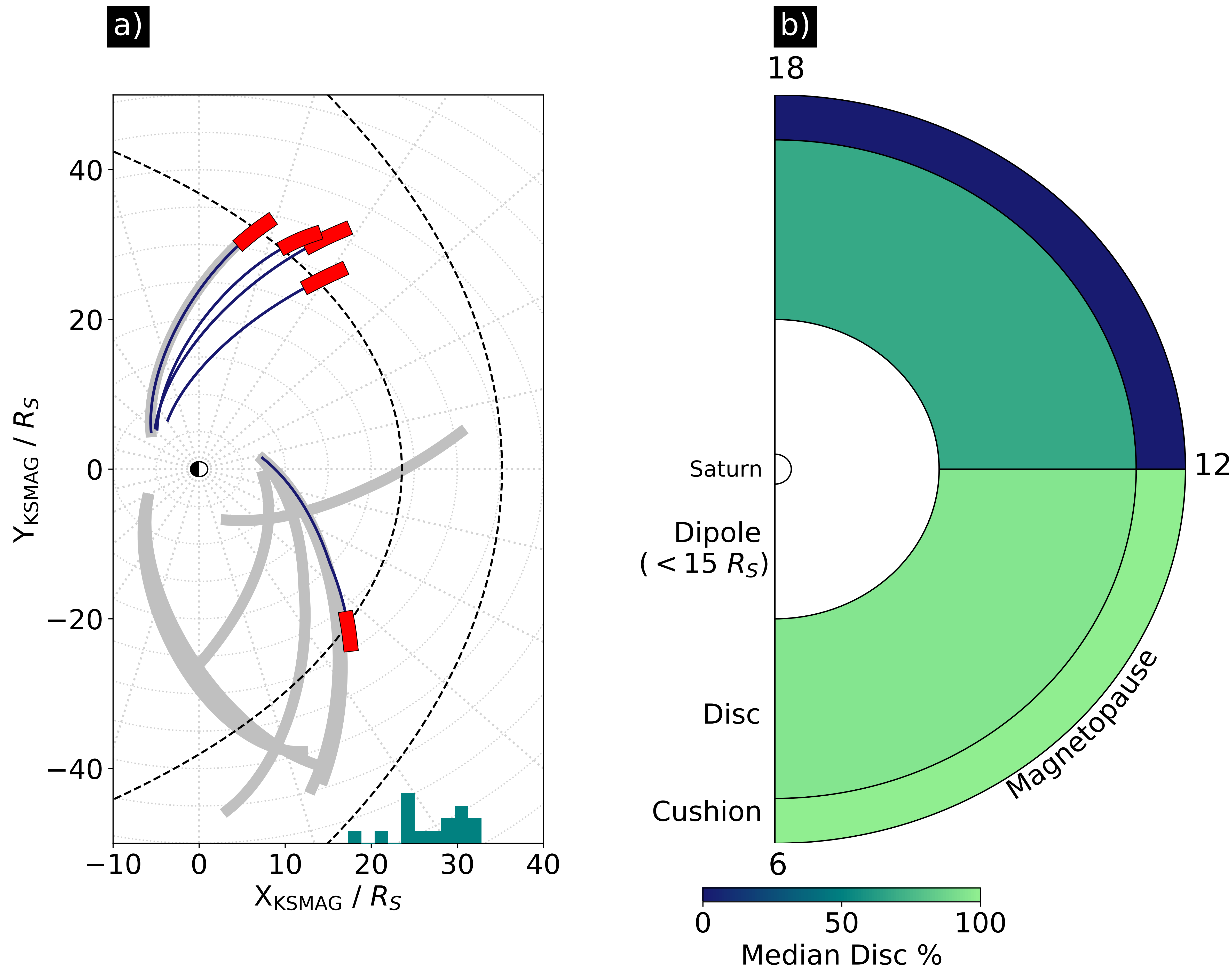
a)
b)
40
20
0
−20
−40
Y_{KSMAG} / R_S
−10
0
10
20
30
40
X_{KSMAG} / R_S
18
12
6
Saturn
Dipole
(< 15 R_S)
Disc
Cushion
Magnetopause
0
50
100
Median Disc %

Figure 4.

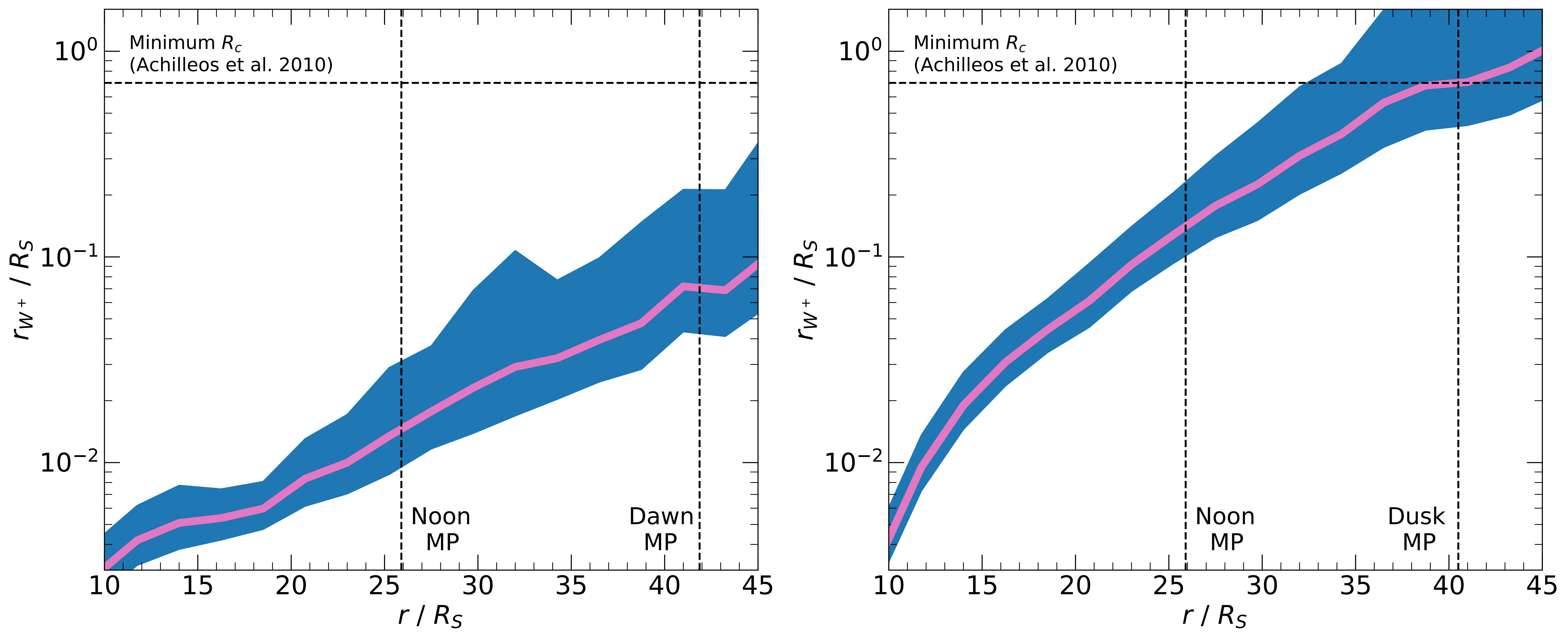

Minimum R_c
(Achilleos et al. 2010)
Noon MP
Dawn MP
Dusk MP
r_{W^+} / R_S
r / R_S
10^0
10^{-1}
10^{-2}
10
15
20
25
30
35
40
45